JOURNAL OF INFORMATION SCIENCE AND ENGINEERING 36, 217-229 (2020)
DOI: 10.6688/JISE.202003_36(2).0003

Investigation of Corrosion Behavior of Carbon Steel for Petroleum Pipeline Applications under Turbulent Flow Conditions

MOHAMMED AHMED[1,2,+], NAYYEF TALIB[1,3] AND LAYTH AL-GEBORY[1,4]
[1]*Faculty of Engineering, Mechanical Engineering Department*
Ozyegin University
Istanbul, 34794 Turkey.
[2]*College of Engineering*
Tikrit University
Tikrit, 34001 Iraq
[3]*College of Engineering*
University of Diyala
Diyala, 32001 Iraq
[4]*Department of Materials Engineering*
University of Technology
Baghdad, 10066 Iraq
[+]*E-mail: salih.ahmed@ozu.edu.tr*

This study investigates the corrosion of steel samples immersed in water with a dynamic corrosion setup at different pH values for three different velocities and three different exposure time. The characteristics of material surface were observed by utilizing Atomic Force Micrographs (AFM). Under the dynamic and static conditions, the rate of corrosion of the steel samples in deionized water (DIW) was calculated through the weight loss measurements. It has been found that the corrosion rate of steel samples under static conditions was higher with the lower pH values. It was observed that the corrosion rate was maximum at pH = 4 and the minimum at pH = 6. The static corrosion tests suggest that the corrosion rate was high in the first two days then decreased with the increasing of time of tests. The effect of wall shear stress and time of immersion was evaluated under the dynamic corrosion tests. The results suggest that increased wall shear stress lead to an increase the corrosion rate specially at pH = 4.

Keywords: material corrosion, immersion tests, wall shear stress, electrochemical analyses, material surface roughness

1. INTRODUCTION

Carbon steel pipelines are commonly used in petroleum industry, for transporting the products, because of their good mechanical properties, low cost and wide availability, despite having low corrosion resistance [1]. Corrosion of pipelines in petroleum industry is not only an economic loss but also a dangerous mode of failure, puts the safety of resources at risk. Corrosion of pipelines occurs due to an electrochemical reaction occurring at the surface of the pipeline in the presence of an electrolyte in an aqueous media, usually soil water [2, 3].

There are several factors that influence the rate of corrosion such as humidity, ionic

Received September 10, 2019; revised September 17, 2019; accepted October 11, 2019.
Communicated by Osamah Ibrahim Khalaf.

strength of the electrolyte environment, the type of metal and the relative movement between the corroding environment and the metal [4]. In petroleum industry pipelines the corrosion is mainly affected by fluid flowing inside the pipelines, this corrosion type is often referred to as flow-dependent corrosion [5-7]. Although fluid hydrodynamics play an important role in flow induced corrosion, the corrosive nature of the fluid is also a factor that should be taken into consideration. The fluid flow may be either laminar or turbulent, which determined by the value of the Reynolds number (Re).

The rate of corrosion gradually increases when the flow velocity increases because the high flow rate leads to higher levels of disturbance and increases the mass transfer rates of the corrosive species from the bulk solutions to the steel surface [8]. An another important factor influencing the rate of flow induced corrosion is Wall Shear Stress (WSS), which expresses the force per unit area exerted by the fluid on the solid boundary [9-11]. The correlation between the flow rate and the WSS for a single phase flow is well known and is best expressed in terms of non-dimensional parameters *i.e.* Reynolds number (*Re*) and the Fanning friction factor (C_f), as given in equation 1 below [12].

$$\{C_f = 0.079Re^{-0.25}\} \tag{1}$$

WSS from the friction factor is calculated as:

$$\{\tau = \frac{\rho C_f V^2}{2}\} \tag{2}$$

where ρ is fluid density (kg.m^{-3}); V is mean flow velocity (m.s^{-1}) and τ is wall shear stress (N.mm^{-2}).

Supat and co-authors examined the influence of the pH on corrosion product layer formation in a controlled water chemistry system. In their study, similar corrosion products characteristics and corrosion rates were observed. It was found that a higher solution pH is likely to give a slightly better protection to the steel surface [13, 14].

Heyn and co-workers found that increasing flow velocity results in a sudden increase in the corrosion rate [15]. The effect of the surface finish of steel sample was investigated by Russel and found that in case of unclean or rusted steel, the rate of corrosion increases continually up to maximum flow velocity [16]. The passivation occurring on the surface of the steel, and the resulting low corrosion rate, can be attributed to the formation of the oxide layer on the surface. This oxide layer works as a protective film against corrosion and as a result, the corrosion rate decreases [17]. Rabald and co-authors, studying the effect of flowing tap water and distilled water on the corrosion rate of steel and cast iron, found that in flowing tap water cast iron corroded faster than steel while in distilled water, it corroded about 300 times faster [18].

Seheers utilized a rotating-cylinder electrode (RCE) to simulate the effect of flow velocity on the pipe corrosion and found higher corrosion rates at lower pH values [19]. Fredj and Burleigh observed very high initial corrosion rate and rapid decrease after a few hours in a high purity deionized water with oxygen. They also found increased corrosion rate at higher velocities even after 7 days of immersion tests but with a lower slope [20]. Several researchers have studied the effect of flow velocity and pH on the rate of corrosion in different media. Table 1. Provides a brief insight into the literature available.

Table 1. Corrosion rate and WSS available in literature.

Reference	Materials	Medium	Time (Hours)	Methods	pH	CR (mm/year)	WSS ($N/m^{2)}$
[19]	Mild steel	Mine water	0.5	RCE Flow loop	7 7	7 8 9 5 6 7.25	0.907 1.844 3.05 0.907 1.844 3.05
[21]	X65	Carbon dioxide environments	24	RCE	4	1	0.8
					5	0.5	2
					6	0.4	6.8
				Flow loop	4	1.05	0.6
					5	0.47	1.2
					6	0.38	5
[22]	X52 steel	NACE 3.5NaCl	24	RCE	4.2 4.1	064 1.1	5.06
[23]	X70 steel	Brine prepared according to NACE standard 1D-196	0.5	RCE	3.89	12.2 at V=1m/s 14.25 at V=3.74m/s	2.64 26.56
[24]	N80 steel	oilfield simulated extraction liquid containing CO2 and HAC	Not available	DF-101S collector magnetic stirrer	Not available	4.676	1.162

Despite the availability of a great deal of literature, there is a gap in understanding the corrosion in pipe flow in terms of wall shear stress, pH and exposure time. For an in-depth understanding of corrosion in petroleum pipes, a combination of parameters such as the generated wall shear stress, range of pH values, and various exposure time needs to be investigated. This work takes into accounts all the above parameters and their effect on the corrosion rate of carbon steel in DI water pH 4-7. The corrosion has been studied with an experimental setup to imitate the real behavior of corrosion in pipe flow. The experiments were conducted over a range of wall shear stress which represents flow in an Iraqi oil field. The dynamic corrosion rate was determined via weight loss measurements. Furthermore, the surface roughness of the steel samples after the electrochemical analysis was investigated using Atomic Force Micrography (AFM).

2. MATERIALS AND METHODS

The carbon steel having composition given in Table 1 used in this study was obtained from Al AHDAB Iraqi Oil Field Company in the form of pipe. The specimens with 10*10*2 mm^2 dimensions were cut from the pipe using electric discharge machine. The surface was initially smoothened with 180-grit SiC paper and then polished with 320, 400, 600, 1000 grit silicon carbide paper until previous coarse scratches were removed. All the experiment tests were done using DIW at different pH values adjusting by adding 0.01M HCl and/or 0.01NaOH.

Table 2. Chemical composition (wt.%) of steel sample.

elements	C	Si	Mn	P	Cr	Mo	Fe
%	0.0946	0.0204	0.903	0.00054	0.0353	0.0222	Balance

2.1 Electrochemical Analysis Methods

Potentiostatic scans and potentiodynamic polarization techniques were utilized to understand the electrochemical behavior of the corrosion of carbon steel. DI water at different pH values was used as electrolyte. The pH values of the electrolyte were adjusted to the desired values using 0.01 M HCl and/ or 0.01M NaOH. All electrochemical measurements were performed with a three electrodes cell in a Gamry 1000 Interface potentiostat. Saturated calomel electrode (SCE) was used as reference, a helical platinum wire as counter electrode and steel sample was used as working electrode,

(A) Potentiostatic (Current vs. Time) Scans

The time period for potentiostatic scan was set to 1800 seconds with an input potential of 0V vs. Eref (the real value shown during the test were ~90-100 μV which was negligible and assumed to be zero). The total volume of electrolyte used was 200ml.

(B) Atomic Force Micrography

Atomic Force Micrographs (AFM) were taken to evaluate the average surface roughness of the steel samples after potentiostatic tests. Three images were taken for a scan area of 10*10μm with scan speed of 6μm for each sample.

(C) Potentiodynamic Polarization

Potentiodynamic analyses of the samples were done in DIW with different pH values. The Potentiodynamic polarization data were measured through changing the electrode potential automatically from −500mV to 1600mV at a sweep rate 1mV.s^{-1}. The tests were done at room temperature.

2.2 Static Corrosion

The static corrosion of the samples was studied by dipping samples as shown in Fig. 1 for 7 days in DIW having different pH values. The corrosion rate was measured by the measuring weight loss every 24 hours. The weight loss was measured with Swiss-Made ES125SM model high precision scientific balance (0.01 mg accuracy). Corrosion rates of carbon steel were calculated by expression:

$$\{V_a = C \times \frac{W_o - W}{\rho A t}\} \tag{3}$$

where, V_a is the corrosion rate or the annual speed, mm/y, C is the conversion factor, which is equal to 8.76×10^4, W_o is weight of specimen before test(g), W is weight of specimen after test(g), ρ is the density of the sample, which is equal (7.85g.cm^{-3}), A is working area of the specimen (cm^2), t is the testing time (hour).

2.3 Dynamic Corrosion

The dynamic corrosion was experimentally measured with the flow loop shown Fig. 1. The setup consists of tank (1), an electrical pump (2), a digital flowmeter (3), steel samples (4) and a regulator (5). The flow meter was utilized to measure the flow rate and a pump for providing flow energy to the fluid. The experiments were conducted at three flow rates and 4 pH values. All the tests were conducted at room temperature. Each test was repeated three times samples. Therefore, the result of each test case is averaged over 9 samples. The corrosion rate was calculated by weight loss measurement using Eq. (4).

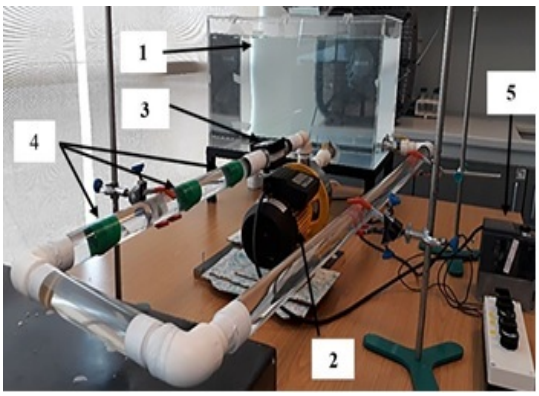

Fig. 1. Experimental setup of dynamic corrosion testing: (1) Tank; (2) Electric pump; (3) Digital flow meter; (4) Steel samples; (5) Regulator.

The flow velocity was calculated from the equation of flow rate as follows,

$$\{V = \frac{Q}{A}\} \tag{4}$$

where Q is the flow rate ($m^3.s^{-1}$), A is the cross section area of the pipe (m^2), and V is the flow velocity ($m.s^{-1}$). The flow velocity, the Reynolds numbers, the Fanning friction factor and WSS for each case were calculated as shown in Table 2. Table 2 provides as comparison of the calculated wall shear stress in our developed setup with WSS calculated in Iraqi oil field.

It can be seen from Table 2 that the calculated wall shear stress from the experimental setup was in close agreement with calculated wall shear stress in the Iraqi oil field. This calculation expected to help in mimicking the real pipe flow corrosion behaviors in real applications.

Table 3. Wall shear stress calculation.

Flow velocity ($m.s^{-1}$)	Reynolds number (Re)	Friction factor (C_f)	WSS(experimental set up (N/mm^2))	WSS (Iraqi oil field (N/mm^2))
0.55	$1.854*10^4$	$6.77*10^{-3}$	1.012	0.5692
0.74	$2.494*10^4$	$6.2286*10^{-3}$	1.716	1.154
0.96	$3.236*10^4$	$5.893*10^{-3}$	2.707	1.914

3. RESULTS AND DISCUSSION

3.1 Electrochemical Evaluation

(A) Potentiostatic Scan

Fig. 2 illustrates the potentiostatic scans of the samples in DIW at different pH values. Generally, carbon steel shows a passive behavior, that is, it becomes covered by an oxide layer that protects it from corrosion. However, in the acidic medium, that passive layer formation is not promoted and the surface is prone to corrosion and with the increasing time of exposure higher current has been observed. Also, it has been noticed that a sharp increase of current with increasing time at pH 4 which indicate that the corrosion rate still increases with time, while at pH 7 there is a slight increase of the current with time at the beginning, then fluctuating increment in pH 7 and then it goes to a near steady state with time which indicate that the corrosion rate in this case near be stable with time. Moreover**,** there is an increase of the current during the test with time at pH 5 but with a lower slope than pH 4 on the other hands, in a case of pH 6 it changes with constant slope along the time which indicate the corrosion rate in this case is minimium which means that there is a protective layer formed on the steel surface. These results show a high degree of congruence with the results obtained through the potentiodynamic polarization as shown in Fig. 5 below.

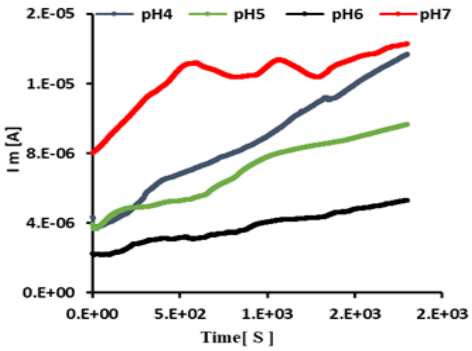

Fig. 2. Potentiostatic (I_m vs time) of steel samples at different pH values.

(B) Atomic Force Microscopy

The surface morphology of the steel samples was examined via Atomic Force Microscopy (AFM) after potentiostatic tests. Figs. 3 (a) and (b) illustrate the surface roughness and the 3D images after potentiostatic scans at different pH values. It can be seen that the average roughness decreases with the increase in pH values. The decrease in roughness can be contributed to the formation of a uniform oxide layer on the surface as we go from acidic to basic environment. However, the presence of a layer of corrosion products causes some surface roughness [19].

(C) Potentiodynamic Polarization

Fig. 4 illustrates potentiodynamic polarization curves of steel samples immersed in

DIW having pH 4, 5, 6 and 7. The electrochemical parameters such as corrosion potential (E_{corr}), I_{corr} and corrosion rate in (mm/year) are presented in Table 2. I_{corr} was calculated through a series of steps involving the Tafel constants β_a and β_c, respectively, to calculate the corrosion rate of the sample [25]:

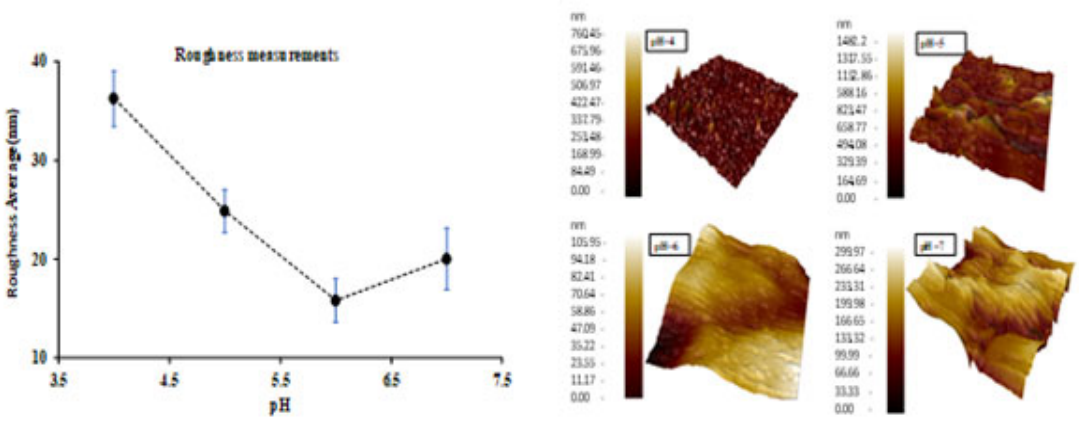

(a) (b)

Fig. 3. (a) Root mean square (RMS) surface roughness measurements of the steel samples treated by static corrosion at PH = 4, pH = 5, pH = 6 and pH = 7; (b) AFM surface micrographs of the samples treated at pH = 4, pH = 5, pH = 6 and pH = 7.

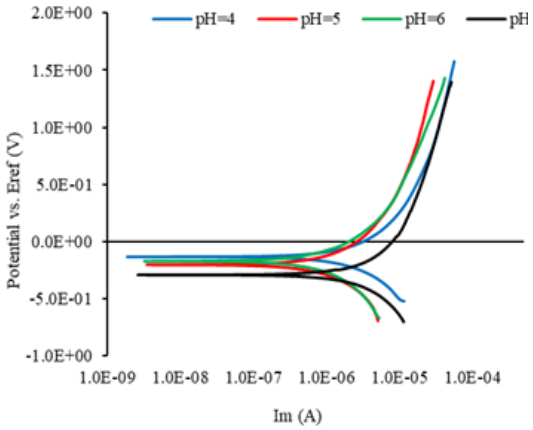

Fig. 4. Potentiodynamic polarization curves of steel samples at different pH values.

$$\{I_{corr} = \frac{\beta_a}{2.3(\beta_a + \beta_c)} \frac{\Delta I}{\Delta E}\}. \tag{5}$$

The corrosion rate was evaluated using the expression [26].

$$\{corrosion\ rate(CR) = \frac{0.13 I_{corr}(E.W)}{density}\} \tag{6}$$

where E.W. is the equivalent weight, I_{corr} is the current density in μA/cm^2, the density of corroding species in g/cm^3, and $\frac{\Delta I}{\Delta E}$ is the slope of the polarization resistance plot, where ΔE is expressed in volts and ΔI is expressed in μA.

From the table it is clear that the rate of corrosion increases as we go from basic to acid environments. The lowest corrosion was observed at pH 6 due to growth of oxide layer on the steel surface, which protected the surface and minimizing the corrosion. On the other hand, pH 7 shows high corrosion value in spite natural or basic medium. Also, pH 4 shows high corrosion rate and it is still high with the increasing of potential.

Table 4. Tafel plot data of steel sample obtained based on potentiodynamic data analyses.

Tafel plot variables	pH = 4	pH = 5	pH = 6	pH = 7
$I_{corr}(\mu A)*10^{-6}$	18,20e-6	25,20e-6	7,610e-6	15,80e-6
$E_{corr}(mV)$	–133.0	–206.0	–172.0	–290.0
CR (mm/year)	8.353	11.84	3.579	7.253

3.2 Static Corrosion

Fig. 5 illustrate the relationship between the corrosion rate and the time of immersion. It can be observed that the corrosion rate is high after the first 24 hours for all the samples and decreases by the increasing of the time of immersion because of the passive layer formation on the surface of the metal, which prevented it from further attack. Similar behavior was observed by S. Peng [27] The steady increase in the rate of corrosion at the beginning in the region of active corrosion was caused by the high interaction between the metal surface and the medium. Moreover, in the range pH 4-7 the behavior of all samples at the beginning was quite similar. After two days of immersion a decrease in corrosion has been observed which is a result of an increase in the formation of corrosion products over time. Since the corrosion tests of this part under study are conducted in static conditions, so this layer grows thicker over time and thus the corrosion rate decreases [28].

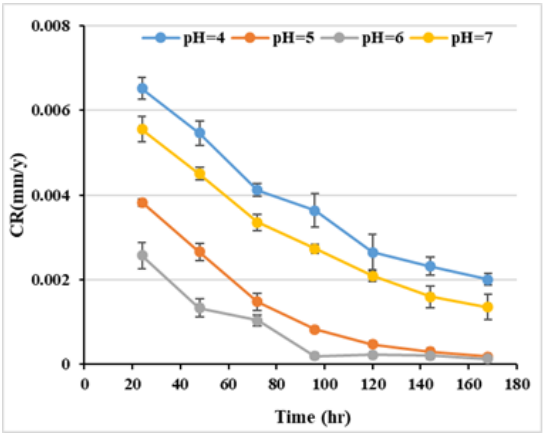

Fig. 5. static corrosion measurements of steel samples at different pH values.

3.3 Dynamic Corrosion

Turbulent flow usually affects the surface water chemistry by changing the mass transfer rate of species moving from the bulk to the steel surface and/or vice versa [29, 30]. Figs. 6-8 show the dynamic corrosion results for steel samples in a range of flow velocities of DIW at different pH values. It can be observed that the rate of corrosion increases with increasing flow velocity. In other words, increasing the wall shear stress along the wall increase the rate of corrosion as shown in Fig. 6. This variation by the dependence of the corrosion rate on the flow velocity is generally attributed to a change by the corrosion mechanism [31].

Higher corrosion rates were observed when the testing time was increased. It can be seen that the corrosion rate at 0.25 m/s reached 0.005 mm/year after 3.30 hours while it reached 0.015 after 10.30 hours at the same velocity as shown in Figs. 6 and 8, this gives indication that increasing time test leads to an increase in the corrosion rate specially in the acidic medium. Moreover, it can be seen that in case of dynamic corrosion tests a decrease in the value of pH leads to an increase in the corrosion rate and this is evident with the value of pH=4. These results are in a good agreement with those of Rhee [14]. The corrosion behavior of the steel samples at pH=7 is similar to the behavior at pH=4 in all times and velocities except that corrosion rate at pH=4 is higher than in pH 7 as shown in Figs. 6-8. However, at pH=6 corrosion is lowest as shown in Fig. 7. This gives an indication that there is an access amount of corrosion products growing on the steel surface and these products are denser and work as a protective layer against corrosion.

The highest corrosion rate was observed at pH=4 and is further accelerated by the increasing velocity as a result of higher interactions between the WSS and the steel surface. The results showed that the corrosion at high velocity but short time give corrosion value less than the value when the time is long as we can see in all the figures. The value reached 0.015 mm/year at time 3.30 hours with velocity 0.96m/s while it reached 0.025 mm/year at time 10.30 hours at the same velocity which can be attributed to the combined effect of the flow velocity over longer periods of time as shown in Fig. 6 and 8. Similar behavior was by Seheers [19], Fredj and Burleigh [20], Z. Li [31] and Young [33].

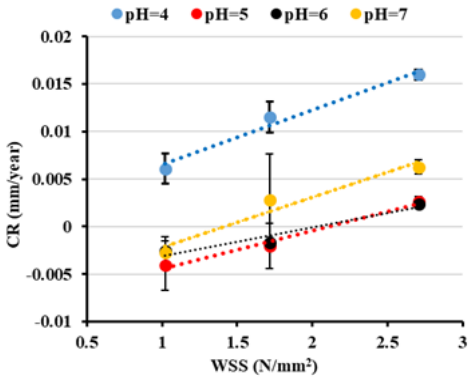

Fig. 6. The relation between corrosion rate and wall shear stress with different pH values after 3.30 hours.

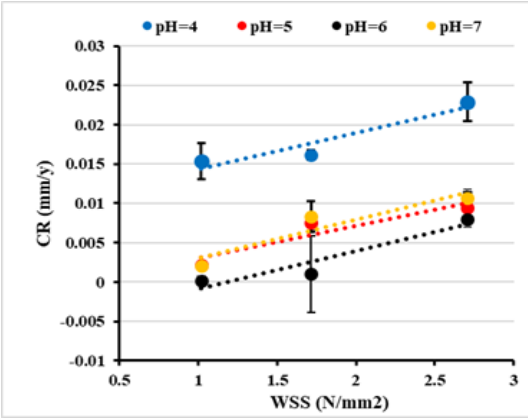

Fig. 7. The relation between corrosion rate and wall shear stress with different pH values after 7 hours.

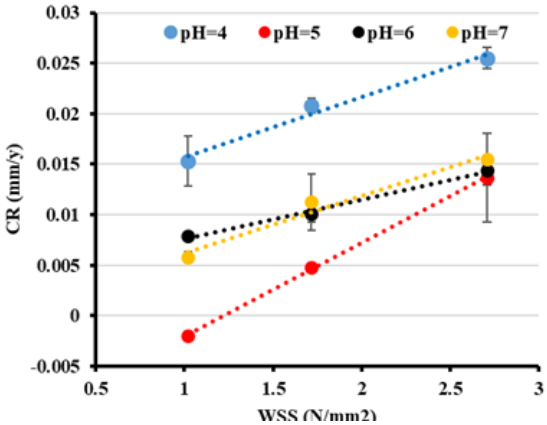

Fig. 8. The relation between corrosion rate and flow velocity with different pH values after 10.30 hours.

From mechanic's point of view increasing the flow rate increases the friction force and has a significant impact on the surface of the sample installed on the surface of the tube, in the developed setup this means increasing turbulence and finally the mass transfer of the corrosive species from the bulk to the pipe wall which may result in an increase in the rate of corrosion. Moreover, the increased turbulence in the bulk as a result of a high flow rate will bring the faster moving fluid closer to the wall (making the boundary layer thinner), results in a higher velocity gradient and higher wall shear stress [10, 20]. The interaction between the surface of the metal and the acid media led to the formation of a visible thin layer on the surface but the increase in WSS as a result of increasing flow velocity leads to the breakage of this layer and which increases the rate of corrosion, this phenomenon was observed for 3.50 hours' tests. As a result of a corrosion, a thin layer forms on the surface of the metal which leads to an increase in the weight of the sample and this was evident even at low velocity specially at pH=5.

4. CONCLUSIONS

In this experimental work, static and dynamic corrosion were studied through an experimental set up to evaluate the effect of flow velocity and wall shear stress with different pH values from acid to basic on the corrosion behavior of steel samples.

In static tests, it is concluded that the corrosion rate decreases with increasing time and it was high in the first two days of the test then it decreases after that, but the acidic medium still has the high corrosion rate. Moreover, in the active corrosion region the corrosion rate was high for all samples in the static tests. The potentiodynamic polarization measurements suppose that the corrosion rate decreases with the increase of pH values. AFM measurement shows that the average roughness decreases with the increasing of pH values and vice versa because of the type of corrosion products formed on the sample's surface.

This study concludes that increasing WSS as a result of flow velocity increases the

corrosion rate for different time tests. Increasing flow rate with pH 4 medium leads to increased corrosion rate as compared to medium with pH 7. Increasing the testing time causes an increase in the corrosion rate in both high and low velocity.

REFERENCES

1. H. M. Tawancy, M. L. Al-Hadhrami, and F. K. Al-Yousef, "Analysis of corroded elbow section of carbon steel piping system of an oil-gas separator vessel," *Case Studies in Engineering Failure Analysis*, Vol. 1, 2013, pp. 6-14.
2. Y. F. Cheng, *Stress Corrosion Cracking of Pipelines*, Vol. 15, John Wiley & Sons, Hoboken, NJ, 2013.
3. D. A. Jones, *Principles and Prevention of Corrosion*, 2nd ed., Prentice Hall, Upper Saddle River, NY, 1996, pp. 168-198.
4. G. Rodriguez, J. Genesca, J. M. Flores, and R. D. Romero, "Electrochemical evaluation of aminotriazole corrosion inhibitor under flow conditions," *Journal of Applied Electrochemistry*, Vol. 39, 2009, pp. 1809-1819.
5. R. Nyman, S. Erixon, B. Tomic, and B. Lydell, "Reliability of piping system components," *SKI Report*, Vol. 95, 1995, p. 58.
6. K. D. Efird, E. J. Wright, J. A. Boros, and T. G. Hailey, "Correlation of steel corrosion in pipe flow with jet impingement and rotating cylinder tests," *Corrosion*, Vol. 49, 1993, pp. 992-1003.
7. J. Weber, "Flow induced corrosion: 25 years of industrial research," *British Corrosion Journal*, Vol. 27, 1992, pp. 193-199.
8. K. D. Efird, "Disturbed flow and flow-accelerated corrosion in oil and gas production," *Journal of Energy Resources Technology*, Vol. 120, 1998, pp. 72-77.
9. R. H. Hausler, C. Consulta, and G. Schmitt, "Hydrodynamic and flow effects on corrosion inhibition," in *Corrosion NACE International*, 2004, pp. 1-20.
10. K. D. Efird, "Jet impingement testing for flow accelerated corrosion," in *Corrosion NACE International*, 2000, pp. 1-26.
11. C. J Chia, F. Giralt, and O. Trass, "Mass transfer in axisymmetric turbulent impinging jets," *Industrial & Engineering Chemistry Fundamentals*, Vol. 16, 1977, pp. 28-35.
12. V. C. Patel and M. R. Head, "Some observations on skin friction and velocity profiles in fully developed pipe and channel flows," *Journal of Fluid Mechanics*, Vol. 38, 1969, pp. 181-201.
13. M. A. Quraishi, J. Rawat, and M. Ajmal, "Synergistic effect of iodide ions on inhibitive performance of substituted dithiobiurets during corrosion of mild steel in hot hydrochloric acid," *Corrosion*, Vol. 55, 1999, pp. 919-923.
14. H. Rhee, H. Jung, and D. Cho, "Evaluation of pH control agents influencing on corrosion of carbon steel in secondary water chemistry condition of pressurized water reactor," *Nuclear Engineering and Technology*, Vol. 46, 2014, pp. 431-438.
15. E. Heyn and O. Bauer, "Einfluß der Temperatur auf die Flußstahlkorrosion," *Mitt. Kgl. Materialprüfungsamt*, Vol. 28, 1910, p. 102.
16. R. P. Russell, E. L. Chappell, and A. White, "Effect of velocity on corrosion of steel under water," *Industrial & Engineering Chemistry*, Vol. 19, 1927, pp. 65-68.

17. M. G. Fontana, *Corrosion Engineering*, Tata McGraw-Hill Education, New Dehli, India, 2005.
18. E. Rabald, *Corrosion Guide*, Elsevier Publishers, Amsterdam, 1968.
19. P. V. Scheers, "The effects of flow velocity and pH on the corrosion rate of mild steel in a synthetic mine water," *Journal of the Southern African Institute of Mining and Metallurgy*, Vol. 92, 1992, pp. 275-281.
20. N. Fredj, T. D. Burleigh, K. L. Heidersbach, and B. R. Crowder, "Corrosion of carbon steel in waters of varying purity and velocity," in *Corrosion NACE International*, 2012.
21. S. Nešic, G. T. Solvi, and J. Enerhaug, "Comparison of the rotating cylinder and pipe flow tests for flow-sensitive carbon dioxide corrosion," *Corrosion*, Vol. 51, 1995, pp. 773-787.
22. R. G. Martinez, J. M. Flores, R. D. Romero and J. G. Llongueras, "Effects of turbulent flow on the corrosion kinetics of X52 pipeline steel in aqueous solutions containing H2S," *Materials and Corrosion*, Vol. 55, 2004, pp. 586-593.
23. A. C. Tobón, M. D. Cruz, J. G. Velázquez, J. G., Salcedo, and R. M. Salinas, "Comparative study on rate of flow accelerated corrosion (FAC) of API 5L X-52-65-70 steels in a brine added with H2S at 60 C by using a rotating cylinder electrode (RCE)," *International Journal of Electrochemical Science*, Vol. 9, 2014, pp. 6781-6792.
24. Q. Niu, Z. Li, G. Cui, and B. Wang, "Effect of flow rate on the corrosion behavior of N80 steel in simulated oil field environment containing CO2 and HAc," *International Journal of Electrochemical Science*, Vol. 12, 2017, pp. 10279-10290.
25. G. Instruments, *Getting Started with Electrochemical Corrosion Measurement*, Warminster, PA, 2011.
26. J. Denny, *Principles and Prevention of Corrosion*, Pearson-Prentice Hall, NJ, 1992.
27. S. Peng and Z. Zeng, "An experimental study on the internal corrosion of a subsea multiphase pipeline," *Petroleum*, Vol. 1, 2015, pp. 75-81.
28. B. O. Hasan and Q. J. M. Slaiman, "The influence of Reynolds number and temperature on the mass transfer coefficient of the corroding pipe," *Journal of Engineering*, Vol. 11, 2005, pp. 741-750.
29. J. Ning, B. Brown, and S. Nesic. "Verification of Pourbaix diagrams for the H2S-H2O-Fe system at 25ºC," in *ICMT Ohio University Advisory Board Meeting*, 2012.
30. S. Nešic, M. Nordsveen, R. Nyborg, and A. Stangeland, "A mechanistic model for carbon dioxide corrosion of mild steel in the presence of protective iron carbonate films – part 2: a numerical experiment," *Corrosion*, Vol. 59, 2003, pp. 489-497.
31. S. Nešić, "Key issues related to modelling of internal corrosion of oil and gas pipelines – A review," *Corrosion Science*, Vol. 49, 2007, pp. 4308-4338.
32. Z. Li, J. Zhang, and J. Cheng, "The influence of critical flow velocity on corrosion of stainless steel," *Journal of Failure Analysis and Prevention*, Vol. 17, 2017, pp. 1234-1240.
33. X. Y. Yong, Y. Q. Zhang, and D. L. Li, "Near the wall of the fluid mechanics, the effect of flow parameters on the corrosion," *Corrosion Protection Technology*, Vol. 3, 2011, pp. 245-250.

Mohammed Salih Ahmed was born in Salahuddin, Iraq. He received his B.Sc. degree in Mechanical Engineering in July 1994 at the University of Technology, Baghdad, Iraq. He got his M.Sc. degree in the Mechanical Engineering in the University of Technology in August 2004. He is currently Ph.D. candidate in Mechanical Engineering / Material Engineering at Özyeğin University, Istanbul, Turkey. His research interests include alloying elements, heat treatments and surface characterization. More specific, chemical mechanical polishing and their application as alternative technique to prevent corrosion in steel pipes. Moreover, organic and an organic coating.

Nayyef Ahmed Talib was born in Diyala, Iraq. He received his B.Sc. degree in Mechanical Engineering in July 1993 at the University of Technology, Baghdad, Iraq. He got his M.Sc. degree in Mechanical Engineering in the University of Technology in August 2001. He got his Ph.D. degree in Mechanical Engineering from Özyeğin University, Istanbul, Turkey in January 2019. He is effective in the field of finite element modelling for polymer processing, material coating, die design, viscoelastic flow modelling. He is a member of Iraqi Engineers Union since 2010.

Layth Wadhah Ismael Al-Gebory was born in Baghdad, Iraq. He received his B.Sc. degree in Mechanical Engineering in July 2000 at the University of Technology, Baghdad, Iraq. He got his M.Sc. degree in Mechanical Engineering in the University of Technology in August 2005. He got his Ph.D. degree in Mechanical Engineering / Nanoparticle suspensions from Özyeğin University, Istanbul, Turkey in August 2018. His research field focuses on the radiative transfer in nanoparticle suspensions. More specific, different issues in the interaction of radiation with nanoparticles and their agglomerates were explained with their applications.